Published in final edited form as:
J Neuropathol Exp Neurol. 2009 September ; 68(9): 994–1005. doi:10.1097/NEN.0b013e3181b44ed8.

Abnormal Localization of Leucine-Rich Repeat Kinase 2 to the Endosomal-Lysosomal Compartment in Lewy Body Disease

Shinji Higashi, MD, PhD[1,2,3], **Darren J Moore, PhD**[4], **Ryoko Yamamoto, MD, PhD**[1,5], **Michiko Minegishi, PhD**[1], **Kiyoshi Sato, MD, PhD**[1], **Takashi Togo, MD, PhD**[6], **Omi Katsuse, MD, PhD**[6], **Hirotake Uchikado, MD, PhD**[6], **Yoshiko Furukawa, MD, PhD**[6], **Hiroaki Hino, MD, PhD**[3], **Kenji Kosaka, MD, PhD**[3], **Piers C. Emson, PhD**[7], **Keiji Wada, MD, PhD**[2], **Valina L Dawson, PhD**[8,9,10,11], **Ted M. Dawson, MD, PhD**[8,9,10], **Heii Arai, MD, PhD**[5], and **Eizo Iseki, MD, PhD**[1]

[1]PET/CT Dementia Research Center, Juntendo Tokyo Koto Geriatric Medical Center, Juntendo University School of Medicine, Koto-ku, Tokyo, Japan [2]Department of Degenerative Neurological Diseases, National Institute of Neuroscience, National Center of Neurology and Psychiatry, Kodaira-shi, Tokyo, Japan [3]Yokohama Houyuu Hospital, Asahi-ku, Yokohama, Japan [4]Laboratory of Molecular Neurodegenerative Research, Brain Mind Institute, Ecole Polytechnique Fédérale de Lausanne, Lausanne, Switzerland [5]Department of Psychiatry, Juntendo University School of Medicine, Bunkyo-ku, Tokyo, Japan [6]Department of Psychiatry, Yokohama City University School of Medicine, Kanazawa-ku, Yokohama, Japan [7]Laboratory of Molecular Neuroscience, The Babraham Institute, Babraham, Cambridge, UK [8]Neuroregeneration and Stem Cell Programs, Institute for Cell Engineering, Johns Hopkins University School of Medicine, Baltimore, Maryland [9]Department of Neurology, Johns Hopkins University School of Medicine, Baltimore, Maryland [10]Department of Neuroscience, Johns Hopkins University School of Medicine, Baltimore, Maryland [11]Department of Physiology, Johns Hopkins University School of Medicine, Baltimore, Maryland

Abstract

Missense mutations in the *leucine-rich repeat kinase 2* (*LRRK2*) gene are the most common causes of both familial and sporadic forms of Parkinson disease (PD) and are also associated with a diverse pathological alterations. The mechanisms whereby *LRRK2* mutations cause these pathological phenotypes are unknown. We employed immunohistochemistry with 3 distinct anti-LRRK2 antibodies to characterize the expression of LRRK2 in the brains of 21 subjects with various neurodegenerative disorders and 7 controls. LRRK2 immunoreactivity was localized in a subset of brainstem-type Lewy bodies (LBs) but not in cortical-type LBs, tau-positive inclusions or TAR-DNA binding protein-43-positive inclusions. LRRK2 immunoreactivity frequently appeared as enlarged granules or vacuoles within neurons of affected brain regions, including the substantia nigra, amygdala and entorhinal cortex in patients with PD or dementia with Lewy bodies (DLB). The volumes of LRRK2-positive granular structures in neurons of the entorhinal cortex were significantly increased in DLB brains compared to aged-matched control brains ($p<0.05$). Double immunolabeling demonstrated that these LRRK2-positive granular structures frequently colocalized with the late-endosomal marker Rab7B and occasionally with the lysosomal marker, LAMP2. These results suggest that LRRK2 normally localizes to the endosomal-lysosomal compartment within morphologically altered neurons in neurodegenerative diseases, particularly in the brains of patients with LB diseases.

Correspondence and reprint requests to: Shinji Higashi M.D., Ph.D. Department of Degenerative Neurological Diseases, National Institute of Neuroscience, National Center of Neurology and Psychiatry, 4-1-1 Ogawa-Higashi, Kodaira-shi, Tokyo 187-8502, Japan. Tel: +81-42-341-2712; Fax: +81-42-346-1745; higashis@ncnp.go.jp.

Keywords

Alzheimer disease; Dementia with Lewy bodies; Endosome; Leucine-rich repeat kinase 2 (LRRK2); Lysosome; PARK8; Parkinson disease

Introduction

Parkinson disease (PD), the second most common age-related neurodegenerative disorder after Alzheimer disease (AD), is characterized by neuronal degeneration with Lewy bodies (LBs) in the substantia nigra pars compacta that leads to dysfunction of the nigrostriatal dopaminergic pathway, striatal dopamine deficiency and clinical parkinsonism. Although the etiology of PD is not known, genetic analysis has provided important new insights into its pathogenesis. Mutations in 6 genes are unambiguously associated with rare Mendelian forms of PD, including *α-synuclein* (1), *parkin* (2), *PTEN-induced putative kinase 1* (*PINK1*) (3), *DJ-1* (4), *leucine-rich repeat kinase 2* (*LRRK2*) (5,6), and *ATP13A2* (7). Of these genes, missense mutations in *LRRK2* have been identified as the cause of late-onset, autosomal dominant parkinsonism linked to chromosome 12q11.2-q13.1 (PARK8 locus). A G2019S mutation in *LRRK2*, which is the most prevalent *LRRK2* variant, also accounts for apparently sporadic cases with PD (8). The disease penetrance in PD subjects with *LRRK2* mutations appears to be age-dependent (9) and their clinical and neurochemical manifestations are not different from those of idiopathic PD subjects. Importantly, in some ethnic subgroups including North African Arabs, Ashkenazi Jews and Arab-Berbers of Tunisia, there is a higher frequency of the G2019S variant in PD cohorts (10,11). Therefore, the LRRK2 protein may provide important insight into the pathogenesis of PD. At present, however, the biological and functional roles of the LRRK2 protein are not well characterized.

In contrast to clinical manifestations that are consistent with idiopathic PD, the brains of patients with *LRRK2* mutations exhibit more diverse pathological alterations. In addition to the classical nigral degeneration predominantly with LB pathology found in the brains of patients with idiopathic PD and dementia with Lewy bodies (DLB) (8,12-15), tau-positive inclusions reminiscent of tauopathies (15,16), ubiquitin-positive pathology only (17), or the distinct absence of pathological inclusions (12,18) are less commonly observed. These findings suggest that LRRK2 may be central to or upstream of pathogenic pathways that regulate α-synuclein or tau protein deposition and that disruptions of this pathway due to *LRRK2* mutations precipitate a PD phenotype. To address this notion, several research groups have investigated the distribution of LRRK2 protein in normal and pathological human brains to determine whether it is localized to LBs or neurofibrillary tangles (NFTs) in synucleinopathies and tauopathies, respectively. The LRRK2 protein has been identified in various brain regions including the striatum, cerebral cortex, hippocampus and cerebellum but at markedly lower levels in the substantia nigra (19-23). Nevertheless, LRRK2 protein is localized to a subset of α-synuclein-positive LBs in the substantia nigra pars compacta of PD and DLB brains (19, 24-27). Furthermore, a previous report showed that diverse tau-positive inclusions in the brains of patients with AD, Parkinsonism dementia complex of Guam, Pick disease (PiD), and amyotrophic lateral sclerosis were immunopositive for LRRK2, suggesting that it may also be localized to tau-positive inclusions in tauopathies and possibly ubiquitin-positive inclusions in TDP-43 proteinopathies (28). In contrast, others have reported that LRRK2 is not localized to NFTs (25). Thus, consistent results regarding the localization of LRRK2 protein in neurodegenerative disorders have not yet been obtained.

In the present study, we investigated a variety of neurodegenerative disorders and found that LRRK2 is localized to a subset of α-synuclein-positive brainstem-type LBs but not to either α-synuclein-positive cortical-type LBs, tau-positive NFTs or other tau inclusions, nor to

TDP-43-positive inclusions. In addition, we often observed LRRK2-positive enlarged granules or vacuoles within neurons of the substantia nigra pars compacta and limbic area of pathological brains (particularly in PD and DLB brains) that are obviously distinct from the smaller LRRK2-positive punctate structures normally present in neurons of control brains. These pathological LRRK2-positive enlarged structures frequently colocalized with the late-endosomal marker, Rab7B, and occasionally with the lysosomal marker, LAMP2. These results suggest a role for LRRK2 in the endosomal-lysosomal system in the pathogenesis of LB diseases.

Materials and Methods

Case Material

We examined 21 postmortem brains from patients with neurodegenerative disorders, including PD, DLB, AD, PiD, progressive supranuclear palsy (PSP), corticobasal degeneration (CBD) and frontotemporal lobar degeneration with ubiquitin inclusions (FTLD-U). The patients had no family history of neurological or psychiatric disorders. Clinical and demographic data are given in Table 1. The PD cases fulfilled the diagnostic criteria for PD (29); DLB cases fulfilled the consensus criteria for a high likelihood of DLB (30); and AD cases fulfilled consensus criteria for a high likelihood of AD (31). The neuropathological features of each case of PD, DLB and AD were assessed as previously described (32) (Table 2). In addition, 7 normal elderly control cases with no previous history of neurological disorders or no evidence of significant neuropathological abnormalities were also studied (Table 1).

Antibodies

Rabbit polyclonal anti-LRRK2 antibodies were generated using KLH-coupled synthetic peptides corresponding to human LRRK2 amino acids 334-347 (JH5517) and 2500-2515 (JH5514), as previously described (35,36). A commercial rabbit polyclonal anti-LRRK2 antibody, NB300-267, was also employed (human LRRK2, amino acids 920–945, Novus Biologicals, Littleton, CO, USA; (37)). These 3 anti-LRRK2 antibodies have previously been shown to recognize a protein band of approximately 280 kDa corresponding to the predicted size of LRRK2 protein by Western blot analysis of cell or tissue lysates, and have been employed in previous studies for immunohistochemistry (12,19,26-28,35-38). Additional antibodies used were anti-phosphorylated α-synuclein (pSer129 (39)), anti-amyloid β, anti-paired helical filament (PHF) tau, anti-TAR DNA binding protein-43 (TDP-43), anti-lysosomal-associated membrane protein 2 (LAMP2), anti-Rab7B, anti-cytochrome oxidase c subunit IV (COX IV), and anti-trans-Golgi network protein 2 (TGOLN2, also known as TGN38) (Table 3).

Immunohistochemical and Immunofluorescent Analysis

Cerebral hemispheres and brainstem, including the midbrain, pons and medulla oblongata, amygdala, hippocampus, entorhinal cortex and inferior temporal cortex (Brodmann area 20), of all brains were fixed in 4% paraformaldehyde in 0.1 M phosphate buffer, pH 7.4 (PBS), embedded in paraffin, and cut into 6-ìm-thick sections. After removal of the paraffin, endogenous peroxidase activity was quenched for 30 minutes with 1.5% H_2O_2 in methanol. Following rehydration, antigens were retrieved with autoclaving or treatment with 70% formic acid. Sections were blocked for 1 hour with 10% normal goat or horse serum and then incubated overnight at 4°C with primary antibodies at the appropriate dilution (Table 3). Sections were incubated for 1 hour with biotinylated secondary antibody, either goat anti-rabbit or horse anti-mouse IgG (1:500, Vector Laboratories, Burlingame, CA), and processed for 45 minutes with avidin-biotin horseradish peroxidase (HRP) complex (ABC) (Vector). Immunoreactivity was visualized with 0.5 mg/ml 3,3,-diaminobenzidine tetrachloride (DAB) and 0.03% H_2O_2. Washes (2 for 20 minutes each) in PBS were carried out between each step. The sections were lightly counterstained with hematoxylin, dehydrated through graded alcohols, cleared with

xylene, and mounted in mounting medium. Some sections were also double-immunostained with antibodies to LRRK2 and either phosphorylated α-synuclein, PHF tau, LAMP2, Rab7B, COX IV or TGOLN2. Immunoreactivity was detected using the ABC-HRP and the ABC-alkaline phosphatase method (ABC-AP Kit) (Vector) and visualized with DAB and fast blue, respectively. The sections were coverslipped with 90% glycerol in PBS.

For double labeling immunofluorescence, the primary antibodies were used at lower dilutions. After incubation overnight at 4°C in antibody to LRRK2 (JH5514, JH5517 or NB300-267; 1:200 dilution) together with antibody to PHF tau, LAMP2, Rab7B, COX IV or TGOLN2, the sections were incubated for 3 hours with AlexaFluor-488 goat anti-rabbit IgG for antibody to LRRK2 and AlexaFluor-594 goat anti-mouse IgG for antibody to PHF tau, LAMP2, Rab7B, COX IV or TGOLN2 (Molecular Probes, Carlsbad, CA). Immunofluorescence was visualized on an Olympus fluoview FV1000 Confocal Microscope.

Morphometric Analysis

For the quantification of the LRRK2-immunoreactive area per cell in 6 DLB, 6 AD and 7 aged control cases, immunohistochemistry was carried out under identical experimental conditions that resulted in comparable background staining intensities among all cases. For each brain, 25 neurons with the nucleolus in focus on the section were selected at random from several fields throughout the entorhinal cortex. Evaluation of LRRK2-immunoreactive areas for each neuron were performed with the Win Roof version 5 (Mitani Corp, Japan) at ×1000 magnification interfaced with an Olympus digital CCD camera (DP71) mounted on an Olympus BX51 microscope. LRRK2-positive enlarged structures were selected as green immunoreactive dots using two-color extraction in the Win Roof program. The areas were then measured. The total cytoplasmic area occupied by faint brown immunoreactivity was also selected as green cytoplasmic area using two-color extraction with similar threshold values in each section followed by the optical dissection of the nucleus if needed, and then the area was quantified. Differences in mean volume of LRRK2-positive enlarged structures among the 3 groups of brains were analyzed by two-tailed unpaired Student *t*-test; p values < 0.05 were considered significant. Measurements of the diameter of LRRK2-positive enlarged structures in the digital images were carried out using the measurement program of line length of the Win Roof software.

Cell Counting

The numbers of neurons with or without enlarged structures, in which LRRK2 immunoreactivity colocalized to Rab-7B immunoreactivity were counted using microscopic fields at ×400 magnification (field size: 0.025 mm^2) in the basal amygdaloid nucleus of DLB brains. The average numbers of neurons in 3 fields were calculated in each DLB case for determining the proportions of neurons with double-positive enlarged structures.

Results

LRRK2 Localizes to Brainstem-type LBs but not to tau- or TDP-43-Positive Pathological Inclusions

We previously reported that a small subset of brainstem-type LBs in the substantia nigra pars compacta in 2 PD cases were immunoreactive for LRRK2 using 2 distinct anti-LRRK2 antibodies (19). Here, we investigated the localization of LRRK2 in the brainstem of 2 PD and 6 DLB cases using 3 anti-LRRK2 antibodies that were raised against distinct LRRK2 peptide sequences (Fig. 1A). LRRK2 immunoreactivity was observed in a small subset of brainstem-type LBs in the substantia nigra pars compacta, locus coeruleus and dorsal vagal nucleus of PD and DLB brains (Fig. 1B–G). The immunoreactivity was predominantly localized to the core (Fig. 1B, D, E, G) or to the rim surrounding the core (Fig. 1C, F) of the LBs; the LB halos

were usually LRRK2-immunonegative. The LRRK2 immunopositivity in these LBs colocalized with phosphorylated α-synuclein (Fig. 1H, I), although the latter was predominant in the halos. Counts in consecutive sections immunostained with 1 of these antibodies indicated that approximately 15% to 40% of phosphorylated α-synuclein-positive brainstem-type LBs are also immunopositive for LRRK2.

By contrast, LRRK2 immunoreactivity in the hippocampus, entorhinal cortex and amygdala from DLB cases did not appreciably colocalize with phosphorylated α-synuclein-positive cortical-type LBs (data not shown). Instead, LRRK2-positive enlarged granular structures were frequently observed in the cytoplasm of neurons in these brain regions (Fig. 1J). Furthermore, LRRK2-positive dystrophic neurites (DNs) were occasionally observed in PD or DLB brain sections immunostained with the LRRK2 antibody NB300-267, but to a lesser extent compared to phosphorylated α-synuclein-positive DNs (data not shown). LRRK2-positive DNs were not usually observed in brain sections immunostained with the anti-LRRK2 antibodies JH5517 and JH5514.

With antibody NB300-267, there was robust LRRK2 immunoreactivty that was frequently observed in obvious tangle-bearing neurons of the hippocampus and entorhinal cortex in a subset of AD cases (Fig. 2B); however, LRRK2 immunoreactivity reminiscent of tau-positive NFTs or DNs was not generally observed in these AD cases using antibodies JH5517 and JH5514 (Fig. 2A). Double immunofluorescent labeling using anti-PHF tau and anti-LRRK2 antibodies (JH5517 and JH5514) revealed that LRRK2 immunoreactivity either does not (Fig. 2D) or only partially (Fig. 2C–E) colocalizes with PHF tau-positive NFTs. We also did not observe LRRK2-positive inclusions in consecutive sections from PiD and CBD brains immunostained for LRRK-2 and tau (Fig 3A–D).

Since tau-negative, α-synuclein-negative, ubiquitin-positive inclusions were reported in brain tissue from a patient with a *LRRK2* mutation (17), we investigated whether LRRK2 localized to TDP-43-positive inclusions in FTLD-U cases,. Neither LRRK2-positive inclusions nor dystrophic neurites were observed in consecutive paired sections of brains of FTLD-U cases immunostained for LRRK2 and TDP-43 (Fig 3E, F).

In summary, these data indicate that LRRK2 is localized to a small subset of brainstem-type LBs but does not localize to other proteinaceous pathological inclusions in the brains of patients with diverse neurodegenerative disorders.

Abnormal Localization of LRRK2 to Enlarged Granules or Vacuoles in Neurons of PD, DLB and AD Brains

LRRK2 immunoreactivity was localized to the neuronal soma and processes in the brains of aged control cases and appeared in a punctate pattern (≤1 μm in diameter) even in regions vulnerable to LB diseases, such as the entorhinal cortex (Fig. 4A) and the substantia nigra pars compacta (Fig 4B). As shown in LRRK2, immunoreactivity frequently localized to numerous dense enlarged granules within neurons of affected regions of DLB brains, such as the entorhinal cortex, amygdala and to a lesser extent, inferior temporal cortex, using the 3 anti-LRRK2 antibodies (Fig. 1J). These enlarged granules were typically ≥1.5 μm in diameter (Fig. 4C) and occasionally greater than 4 μm in diameter (Fig. 4D); they were mostly observed in the neuronal soma but occasionally in neuronal processes. In addition to the enlarged granules, LRRK2 immunoreactivity was often localized to clustered vacuoles in neurons of these limbic regions (Fig. 4E). In PD and DLB brains the LRRK2-positive enlarged structures are also observed in surviving dopaminergic neurons of the substantia nigra pars compacta (Fig. 4F) but they were not observed in nigral dopaminergic neurons in aged control brains (Fig. 4B). In addition, LRRK2-positive enlarged structures in neurons of the entorhinal cortex were also observed in PD (Fig. 4G) and AD brains (Fig. 4H), albeit to a lesser extent compared to DLB

brains. Thus, abnormal neuronal LRRK2 immunoreactivity has similar morphological characteristics in the limbic regions of DLB brains and the substantia nigra pars compacta of PD and DLB brains. Therefore, we speculate that these LRRK2-positive enlarged structures may be pathological features common to LB diseases and possibly also AD.

To evaluate the difference in volume of these abnormal granular structures between DLB and AD, we used computerized morphometry to determine the percentages of total neuronal area occupied by LRRK2-positive granular structures in the entorhinal cortex of brains from DLB, AD and aged control cases. This morphometric analysis enabled a precise estimate of the cell area occupied by granular LRRK2 immunoreactivity (Fig. 4I). The mean percentage of cell area occupied by granular LRRK2 immunoreactivity was significantly increased in DLB brains compared to control brains (DLB, 7.62 ± 0.55% vs. controls, 5.27 ± 0.73% [mean ± S.E.M], $p = 0.026$) (Fig. 4J). In contrast, there was no significant difference between AD and control brains, despite a strong trend towards increased LRRK2-immunoreactive volumes in the AD brains compared to the control brains (AD 7.04 ± 0.26%, $p = 0.057$ vs. controls) (Fig. 4J). We also analyzed the correlation between cell area occupied by LRRK2-positive granular structures and the stage of neurofibrillary and Lewy body pathology using the Spearman rank correlation coefficient but the differences as not significant ($p > 0.05$). The LRRK2-positive enlarged structures were only sparsely observed in brains from PiD, PSP, CBD and FTLD-U cases.

LRRK2-Positive Enlarged Granules or Vacuoles Colocalize with Late-Endosomal and Lysosomal Makers, Rab7B and LAMP2

We next examined the subcellular localization of LRRK2-positive enlarged granules or vacuoles in limbic brain regions from DLB subjects using antibodies to proteins that localize to distinct cytoplasmic organelles. We selected these markers based on the reported localizations of LRRK2 to the Golgi apparatus (35,40), mitochondria (35,36,40), endosomes (35,41) and lysosomes (35,42). LRRK2-positive enlarged granules or vacuoles mostly colocalized with the late endosomal marker, Rab7B (Figs. 5A, 5B, 6A). The proportions of neurons with double-positive granules (LRRK2/Rab7B) in DLB brains varied from case to case: from approximately 5 to 50% (mean ± S.D. 24.6 ± 20.9%). The 2 DLB brains with the most severe Lewy body pathology (stage IV, Table 2) displayed the highest frequency of neurons bearing double-positive granules (49.4 ± 5.9%). Some LRRK2-positive enlarged granules or vacuoles also colocalized with LAMP2-positive lysosomal structures (Figs. 5C, 6B), albeit in less than ~5% of the neurons. In contrast, LRRK2-positive enlarged structures only rarely colocalize with the trans-Golgi marker TGN38 or the mitochondrial marker COX IV (Figs. 5D, E, 6C, D) in neurons of these limbic brain regions from DLB subjects. This indicates that LRRK2 localizes to the endosomal-lysosomal compartment under pathological conditions in Lewy body disease and AD.

Discussion

In the present study, we demonstrate that LRRK2 immunoreactivity colocalizes to a subset of α-synuclein-positive brainstem-type LBs, especially to the inner core and its outer rim of LBs, in PD and DLB brains, whereas α-synuclein immunoreactivity localizes predominantly to the LB halos. In contrast, LRRK2 immunoreactivity does not appreciably overlap with α-synuclein-positive cortical-type LBs and DNs in the cerebral cortex or amygdala of PD and DLB brains. The immunostaining pattern of LRRK2 in Lewy body diseases is clearly distinct from that of α-synuclein, and tends to resemble that of synphilin-1 (43). In contrast to the LB halo, which is composed of Lewy filaments, the core of LBs is mainly composed of densely packed vesicular structures (44). Therefore, we speculate that LRRK2 might localize to

vesicular structures of unknown origin rather than to filamentous aggregates of α-synuclein within LBs, as has also been speculated for synphilin-1 localization (43).

We also found that LRRK2 immunoreactivity did not colocalize with tau-positive NFTs, other tau inclusions, or with TDP-43-positive inclusions in brains of AD, various tauopathies or TDP-43 proteinopathy cases. In AD brains, LRRK2 immunoreactivity did not localize to NFTs when the anti-LRRK2 antibodies JH5517 and JH5514 were used, whereas it localized with a subset of NFTs when the commercial anti-LRRK2 antibody NB300-267 was used. The 3 distinct rabbit polyclonal antibodies to LRRK2 used here were rigorously evaluated in our previous study, in which we show that each antibody can detect endogenous human LRRK2 protein (38). The inconsistent findings between the JH5514 and JH5517 antibodies and the NB300-267 antibody may be due to additional non-specific cross-reactivity of NB300-267 since the JH5514 antibody has been validated using LRRK2 knockout mice and detects endogenous LRRK2 as the major protein species in brain tissue in wild-type control mice (38). We conclude, therefore, that LRRK2 is not a component common to different protein aggregates of these neurodegenerative disorders.

We next examined whether the subcellular localization or expression of LRRK2 is altered under pathological conditions in neurodegenerative disease. We previously reported that LRRK2 localizes exclusively to neuronal membrane-bound and vesicular structures including endosomes, lysosomes, multivesicular bodies, various transport vesicles and mitochondria in vivo (35). In addition, LRRK2 immunoreactivity is morphologically observed as a distinct punctate staining pattern in human and rodent brain tissue and mouse primary cortical neurons (19,35), consistent with the present data in aged human control brains. In the present study, morphological alterations of LRRK2 immunoreactivity were frequently observed as enlarged granules or clustered vacuoles in neurons within the affected limbic areas of DLB brains. Morphometric analysis reveals that the volume of cell area occupied by these LRRK2-positive structures in neurons was elevated in brain regions with Lewy body pathology in DLB compared to similar regions of aged control brains. Recent studies have shown that certain disease-linked mutations in *LRRK2* produce a hyperactive kinase and induce toxicity in primary neurons (36,40,45,46). In addition, autosomal dominant inheritance of *LRRK2* mutations in families with PD is most likely consistent with a gain-of-function mechanism for the pathogenic properties of *LRRK2* mutations (47). Therefore, it is most likely that morphological alterations and increased volume of LRRK2 immunoreactivity may reflect an elevated expression level and thus greater overall kinase or enzymatic activity of LRRK2 per neuron in brain regions with Lewy pathology. At this juncture, however, it is not possible to rule out improved accessibility of LRRK2 epitopes for binding to each antibody that would also result in increased LRRK2 immunoreactivity in brain tissue. This seems unlikely since the 3 antibodies we used detect distinct amino- or carboxyl-terminal epitopes. Because it has been exceedingly difficult to detect full-length LRRK2 in postmortem human samples by Western analysis with numerous LRRK2 antibodies, it is not currently possible to determine whether there is an increase in LRRK2 protein expression in these DLB brain regions. This issue will require further analysis as the tools for detecting LRRK2 improve.

LRRK2-positive enlarged granules or vacuoles frequently colocalized to Rab7B-positive late endosomes and occasionally with LAMP2-positive lysosomes, suggesting that LRRK2 may be associated with the endosomal-lysosomal system in these pathological brains. Growing evidence indicates that the autophagy or lysosomal systems are associated with the pathogenesis of PD, including accumulation of autophagic vacuoles in PD brains (48), clearance of misfolded α-synuclein by autophagy (49-51), and mutations in the lysosomal ATPase *ATP13A2* leading to a parkinsonian phenotype (7). In addition, there is recent evidence of an important role for LRRK2 in the endosomal-lysosomal system. For example, increased autophagic or lysosomal compartments were observed in primary cortical neurons (52) and in

SH-SY5Y cells expressing the *LRRK2* G2019S variant (42). Moreover, LRRK2 is reported to interact with Rab5B, a component of the endosomal pathway that regulates synaptic vesicle endocytosis (41). Shin et al recently demonstrated that LRRK2 overexpression impaired synaptic vesicle endocytosis in rat primary hippocampal neurons, indicating that LRRK2 may influence endosomal pathway function (39). These observations suggest that PD-linked mutations in *LRRK2* may lead to neuronal dysfunction and parkinsonism through perturbations in the endosomal-lysosomal trafficking pathway. Given that LRRK2 is localized to the core of LBs that are typically enriched in vesicular structures as described above, localization of LRRK2 to the endosomal-lysosomal subcellular compartments within neurons suggests that LRRK2 may function as part of the endocytic machinery that normally regulates vesicular trafficking.

Intriguingly, LRRK2-positive enlarged structures are also observed in neurons of the limbic area of AD brains. The volume of cell area occupied by LRRK2-positive structures in neurons of AD brains showed a strong tendency to increase compared to that in aged control brains; however, this was not statistically significant. Involvement of the endosomal-lysosomal system in the pathogenesis of AD is well documented and expression of various endosomal or lysosomal proteins are reported to be increased in neurons in regions affected in AD (53,54). Late endosome/multivesicular bodies contain amyloid-β (Aβ) peptide (55), and intracellular Aβ peptide may be generated in the endosomal compartment by cleavage of amyloid precursor protein (APP) (56). In addition, with reference to abnormalities of the endosomal-lysosomal system in several neurodegenerative disorders (54), recent studies suggest that impaired autophagy through genetic disruption of ATG5 or ATG7 in neurons causes frank neuronal degeneration characterized by ubiquitin-positive inclusions, a pathological feature common to many neurodegenerative disorders (55,56). Thus, disruption of the endosomal-lysosomal system is considered to be a pathogenic event common not only to LB diseases such as PD and DLB, but also to other neurodegenerative disorders including AD, as suggested by our finding of abnormal LRRK2-positive enlarged late endosomal compartments in neurons of the limbic area of AD brains and in DLB brains. Because *LRRK2* mutations usually cause a PD phenotype, however, the involvement of LRRK2 in the pathogenesis of AD may be indirect. It is of great interest to determine whether the function of LRRK2 in the endosomal machinery is associated with the pathogenesis in AD or with the diverse pathology observed in brains with *LRRK2* mutations.

In conclusion, the present observation that LRRK2 is localized only to the core of α-synuclein-positive brainstem-type LBs but not to either α-synuclein-positive cortical-type LBs and DNs, tau-positive NFTs and other inclusions, or TDP-43-positive inclusions, suggests that LRRK2 is not a common cardinal protein component of filamentous proteinaceous aggregates in various neurodegenerative disorders. In addition, morphological alterations and increased volume of LRRK2 immunoreactivity in DLB brains may indicate perturbed expression or enzymatic activity of LRRK2 associated with Lewy pathology and could be associated with a principal pathogenic event that triggers the development of the disease. The present observation that LRRK2-positive granules or vacuoles colocalize with the endosomal-lysosomal compartment may be associated with the pathogenic role of LRRK2 leading to neuronal degeneration. These findings may provide important insight into the contribution of LRRK2 dysfunction to the pathogenesis of LB diseases.

Acknowledgments

We are grateful to the patients and their families who make this research possible. T.M.D. is the Leonard and Madlyn Abramson Professor in Neurodegenerative Diseases at Johns Hopkins.

This research was supported by grants from the Kurata Memorial Hitachi Science and Technology Foundation (S.H.), Grants-in-Aid for Young Scientists (B), 21790856 (S.H.), the Japan Ministry of Education, Science, Sports and Culture

(E. I.), and NIH/NINDS grant NS38377 (T.M.D.) and by funding support from the Ecole Polytechnique Fédérale de Lausanne (D.J.M.).

References

1. Polymeropoulos MH, Lavedan C, Leroy E, et al. Mutation in the alpha-synuclein gene identified in families with Parkinson's disease. Science 1997;276:2045–47. [PubMed: 9197268]
2. Kitada T, Asakawa S, Hattori N, et al. Mutations in the parkin gene cause autosomal recessive juvenile parkinsonism. Nature 1998;392:605–8. [PubMed: 9560156]
3. Valente EM, Abou-Sleiman PM, Caputo V, et al. Hereditary early-onset Parkinson's disease caused by mutations in PINK1. Science 2004;304:1158–60. [PubMed: 15087508]
4. Bonifati V, Rizzu P, van Baren MJ, et al. Mutations in the DJ-1 gene associated with autosomal recessive early-onset parkinsonism. Science 2003;299:256–59. [PubMed: 12446870]
5. Zimprich A, Biskup S, Leitner P, et al. Mutations in LRRK2 cause autosomal-dominant parkinsonism with pleomorphic pathology. Neuron 2004;44:601–7. [PubMed: 15541309]
6. Paisan-Ruiz C, Jain S, Evans EW, et al. Cloning of the gene containing mutations that cause PARK8-linked Parkinson's disease. Neuron 2004;44:595–600. [PubMed: 15541308]
7. Ramirez A, Heimbach A, Grundemann J, et al. Hereditary parkinsonism with dementia is caused by mutations in ATP13A2, encoding a lysosomal type 5 P-type ATPase. Nat Genet 2006;38:1184–91. [PubMed: 16964263]
8. Gilks WP, Abou-Sleiman PM, Gandhi S, et al. A common LRRK2 mutation in idiopathic Parkinson's disease. Lancet 2005;365:415–16. [PubMed: 15680457]
9. Kachergus J, Mata IF, Hulihan M, et al. Identification of a novel LRRK2 mutation linked to autosomal dominant parkinsonism: Evidence of a common founder across European populations. Am J Hum Genet 2005;76:672–80. [PubMed: 15726496]
10. Healy DG, Falchi M, O'Sullivan SS, et al. Phenotype, genotype, and worldwide genetic penetrance of LRRK2-associated Parkinson's disease: A case-control study. Lancet Neurol 2008;7:583–90. [PubMed: 18539534]
11. Hulihan MM, Ishihara-Paul L, Kachergus J, et al. LRRK2 Gly2019Ser penetrance in Arab-Berber patients from Tunisia: a case-control genetic study. Lancet Neurol 2008;7:591–94. [PubMed: 18539535]
12. Giasson BI, Covy JP, Bonini NM, et al. Biochemical and pathological characterization of Lrrk2. Ann Neurol 2006;59:315–22. [PubMed: 16437584]
13. Giordana MT, D'Agostino C, Albani G, et al. Neuropathology of Parkinson's disease associated with the LRRK2 Ile1371Val mutation. Mov Disord 2007;22:275–78. [PubMed: 17149743]
14. Ross OA, Toft M, Whittle AJ, et al. Lrrk2 and Lewy body disease. Ann Neurol 2006;59:388–93. [PubMed: 16437559]
15. Wszolek ZK, Pfeiffer RF, Tsuboi Y, et al. Autosomal dominant parkinsonism associated with variable synuclein and tau pathology. Neurology 2004;62:1619–22. [PubMed: 15136696]
16. Rajput A, Dickson DW, Robinson CA, et al. Parkinsonism, Lrrk2 G2019S, and tau neuropathology. Neurology 2006;67:1506–8. [PubMed: 17060589]
17. Dachsel JC, Ross OA, Mata IF, et al. Lrrk2 G2019S substitution in frontotemporal lobar degeneration with ubiquitin-immunoreactive neuronal inclusions. Acta Neuropathol 2007;113:601–6. [PubMed: 17151837]
18. Hasegawa K, Kowa H. Autosomal dominant familial Parkinson disease: Older onset of age, and good response to levodopa therapy. Eur Neurol 1997;38:39–43. [PubMed: 9276200]
19. Higashi S, Biskup S, West AB, et al. Localization of Parkinson's disease-associated LRRK2 in normal and pathological human brain. Brain Res 2007;1155:208–19. [PubMed: 17512502]
20. Higashi S, Moore DJ, Colebrooke RE, et al. Expression and localization of Parkinson's disease-associated leucine-rich repeat kinase 2 in the mouse brain. J Neurochem 2007;100:368–81. [PubMed: 17101029]
21. Galter D, Westerlund M, Carmine A, et al. LRRK2 expression linked to dopamine-innervated areas. Ann Neurol 2006;59:714–19. [PubMed: 16532471]

22. Taymans JM, Van den Haute C, Baekelandt V. Distribution of PINK1 and LRRK2 in rat and mouse brain. J Neurochem 2006;98:951–61. [PubMed: 16771836]
23. Melrose H, Lincoln S, Tyndall G, et al. Anatomical localization of leucine-rich repeat kinase 2 in mouse brain. Neuroscience 2006;139:791–94. [PubMed: 16504409]
24. Melrose HL, Kent CB, Taylor JP. A comparative analysis of leucine-rich repeat kinase 2 (Lrrk2) expression in mouse brain and Lewy body disease. Neuroscience 2007;147:1047–58. [PubMed: 17611037]
25. Perry G, Zhu X, Babar AK, et al. Leucine-rich repeat kinase 2 colocalizes with alpha-synuclein in Parkinson's disease, but not tau-containing deposits in tauopathies. Neurodegener Dis 2008;5:222–24. [PubMed: 18322396]
26. Zhu X, Babar A, Siedlak SL, et al. LRRK2 in Parkinson's disease and dementia with Lewy bodies. Mol Neurodegener 2006;1:17. [PubMed: 17137507]
27. Zhu X, Siedlak SL, Smith MA, et al. LRRK2 protein is a component of Lewy bodies. Ann Neurol 2006;60:617–618. [PubMed: 16847950]author reply 618-19
28. Miklossy J, Arai T, Guo JP, et al. LRRK2 expression in normal and pathologic human brain and in human cell lines. J Neuropathol Exp Neurol 2006;65:953–63. [PubMed: 17021400]
29. Gelb DJ, Oliver E, Gilman S. Diagnostic criteria for Parkinson disease. Arch Neurol 1999;56:33–39. [PubMed: 9923759]
30. McKeith IG, Dickson DW, Lowe J, et al. Diagnosis and management of dementia with Lewy bodies: third report of the DLB Consortium. Neurology 2005;65:1863–72. [PubMed: 16237129]
31. Consensus recommendations for the postmortem diagnosis of Alzheimer's disease. The National Institute on Aging, and Reagan Institute Working Group on Diagnostic Criteria for the Neuropathological Assessment of Alzheimer's Disease. Neurobiol Aging 1997;18:S1–S2. [PubMed: 9330978]
32. Higashi S, Iseki E, Yamamoto R, et al. Concurrence of TDP-43, tau and alpha-synuclein pathology in brains of Alzheimer's disease and dementia with Lewy bodies. Brain Res 2007;1184:284–94. [PubMed: 17963732]
33. Braak H, Alafuzoff I, Arzberger T, et al. Staging of Alzheimer disease-associated neurofibrillary pathology using paraffin sections and immunocytochemistry. Acta Neuropathol (Berl) 2006;112:389–404. [PubMed: 16906426]
34. Marui W, Iseki E, Kato M, et al. Pathological entity of dementia with Lewy bodies and its differentiation from Alzheimer's disease. Acta Neuropathol (Berl) 2004;108:121–28. [PubMed: 15235805]
35. Biskup S, Moore DJ, Celsi F, et al. Localization of LRRK2 to membranous and vesicular structures in mammalian brain. Ann Neurol 2006;60:557–69. [PubMed: 17120249]
36. West AB, Moore DJ, Biskup S, et al. Parkinson's disease-associated mutations in leucine-rich repeat kinase 2 augment kinase activity. Proc Natl Acad Sci U S A 2005;102:16842–47. [PubMed: 16269541]
37. Greggio E, Jain S, Kingsbury A, et al. Kinase activity is required for the toxic effects of mutant LRRK2/dardarin. Neurobiol Dis 2006;23:329–41. [PubMed: 16750377]
38. Biskup S, Moore DJ, Rea A, et al. Dynamic and redundant regulation of LRRK2 and LRRK1 expression. BMC Neurosci 2007;8:102. [PubMed: 18045479]
39. Saito Y, Kawashima A, Ruberu NN, et al. Accumulation of phosphorylated alpha-synuclein in aging human brain. J Neuropathol Exp Neurol 2003;62:644–54. [PubMed: 12834109]
40. Gloeckner CJ, Kinkl N, Schumacher A, et al. The Parkinson disease causing LRRK2 mutation I2020T is associated with increased kinase activity. Hum Mol Genet 2006;15:223–32. [PubMed: 16321986]
41. Shin N, Jeong H, Kwon J, et al. LRRK2 regulates synaptic vesicle endocytosis. Exp Cell Res 2008;314:2055–65. [PubMed: 18445495]
42. Plowey ED, Cherra SJ 3rd, Liu YJ, et al. Role of autophagy in G2019S-LRRK2-associated neurite shortening in differentiated SH-SY5Y cells. J Neurochem 2008;105:1048–56. [PubMed: 18182054]
43. Wakabayashi K, Engelender S, Yoshimoto M, et al. Synphilin-1 is present in Lewy bodies in Parkinson's disease. Ann Neurol 2000;47:521–23. [PubMed: 10762166]

44. Takahashi H, Wakabayashi K. The cellular pathology of Parkinson's disease. Neuropathology 2001;21:315–22. [PubMed: 11837539]
45. Smith WW, Pei Z, Jiang H, et al. Kinase activity of mutant LRRK2 mediates neuronal toxicity. Nat Neurosci 2006;9:1231–33. [PubMed: 16980962]
46. West AB, Moore DJ, Choi C, et al. Parkinson's disease-associated mutations in LRRK2 link enhanced GTP-binding and kinase activities to neuronal toxicity. Hum Mol Genet 2007;16:223–32. [PubMed: 17200152]
47. Moore DJ. The biology and pathobiology of LRRK2: Implications for Parkinson's disease. Parkinsonism Relat Disord 2008;14:S92–98. [PubMed: 18602856]
48. Anglade P, Vyas S, Javoy-Agid F, et al. Apoptosis and autophagy in nigral neurons of patients with Parkinson's disease. Histol Histopathol 1997;12:25–31. [PubMed: 9046040]
49. Cuervo AM, Stefanis L, Fredenburg R, et al. Impaired degradation of mutant alpha-synuclein by chaperone-mediated autophagy. Science 2004;305:1292–95. [PubMed: 15333840]
50. Lee HJ, Khoshaghideh F, Patel S, et al. Clearance of alpha-synuclein oligomeric intermediates via the lysosomal degradation pathway. J Neurosci 2004;24:1888–96. [PubMed: 14985429]
51. Webb JL, Ravikumar B, Atkins J, et al. Alpha-Synuclein is degraded by both autophagy and the proteasome. J Biol Chem 2003;278:25009–13. [PubMed: 12719433]
52. MacLeod D, Dowman J, Hammond R, et al. The familial Parkinsonism gene LRRK2 regulates neurite process morphology. Neuron 2006;52:587–93. [PubMed: 17114044]
53. Cataldo AM, Barnett JL, Pieroni C, et al. Increased neuronal endocytosis and protease delivery to early endosomes in sporadic Alzheimer's disease: Neuropathologic evidence for a mechanism of increased beta-amyloidogenesis. J Neurosci 1997;17:6142–51. [PubMed: 9236226]
54. Nixon RA, Wegiel J, Kumar A, et al. Extensive involvement of autophagy in Alzheimer disease: An immuno-electron microscopy study. J Neuropathol Exp Neurol 2005;64:113–122. [PubMed: 15751225]
55. Takahashi RH, Milner TA, Li F, et al. Intraneuronal Alzheimer abeta42 accumulates in multivesicular bodies and is associated with synaptic pathology. Am J Pathol 2002;161:1869–79. [PubMed: 12414533]
56. Small SA, Gandy S. Sorting through the cell biology of Alzheimer's disease: Intracellular pathways to pathogenesis. Neuron 2006;52:15–31. [PubMed: 17015224]
57. Martinez-Vicente M, Cuervo AM. Autophagy and neurodegeneration: When the cleaning crew goes on strike. Lancet Neurol 2007;6:352–61. [PubMed: 17362839]
58. Hara T, Nakamura K, Matsui M, et al. Suppression of basal autophagy in neural cells causes neurodegenerative disease in mice. Nature 2006;441:885–89. [PubMed: 16625204]
59. Komatsu M, Waguri S, Chiba T, et al. Loss of autophagy in the central nervous system causes neurodegeneration in mice. Nature 2006;441:880–84. [PubMed: 16625205]

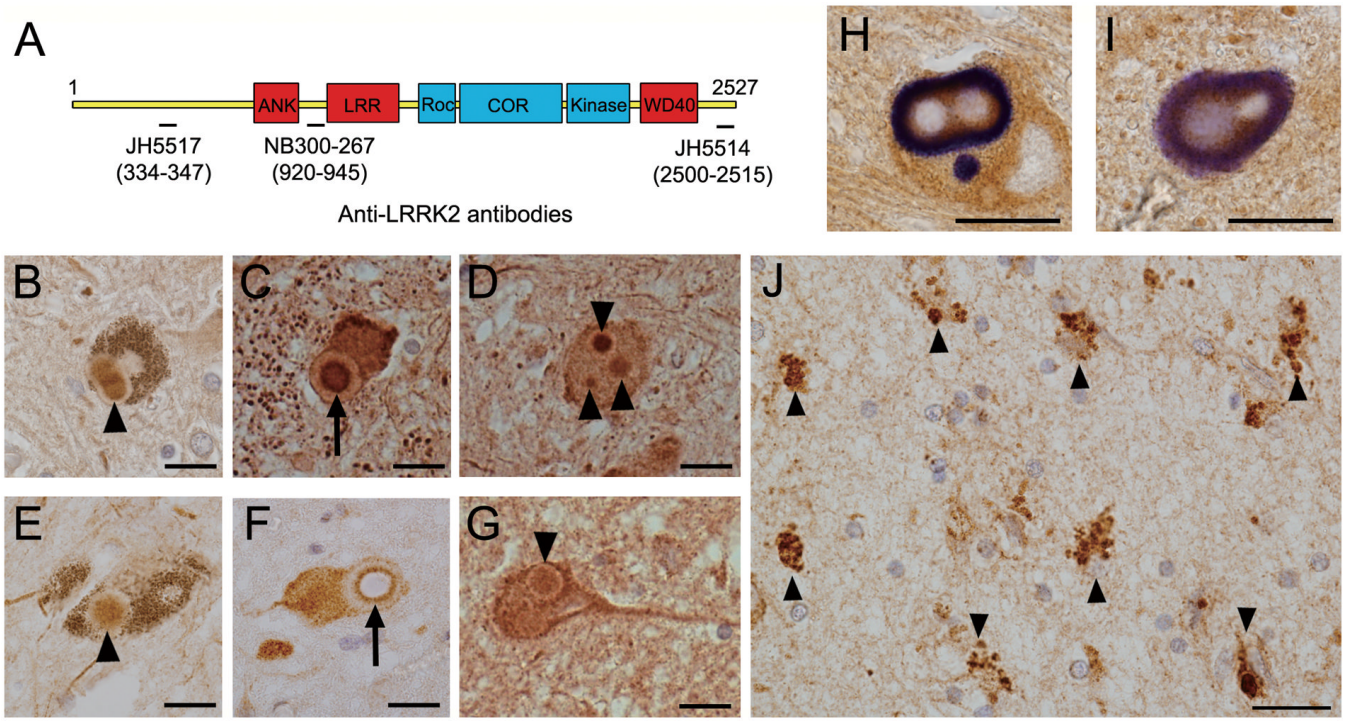

Figure 1.

Localization of leucine-rich repeat kinase 2 (LRRK2) in the brains of Parkinson disease (PD) and dementia with Lewy bodies (DLB) cases. **(A)** The location of peptides recognized by 3 LRRK2-specific polyclonal antibodies are shown aligned to the protein domain structure of LRRK2. **(B-G)** LRRK2 immunoreactivity in the core (arrowheads) and its outer rim (arrows) of brainstem-type Lewy bodies (LBs) in the substantia nigra pars compacta (**B, E**), locus coeruleus (**C, D, G**) or dorsal vagal nucleus (**F**) of PD (**B, C, E, F**) or DLB (**D, G**) brains. **(H, I)** Double immunolabeling for LRRK2 (brown) and phosphorylated α-synuclein (blue) shows colocalization of LRRK2 with α-synuclein-positive brainstem-type LBs (dark brown). **(J)** LRRK2 immunohistochemistry in the amygdala of a DLB brain; LRRK2-positive enlarged granules are observed within the cytoplasm of neurons (arrowheads). Scale bars = 20 μm.

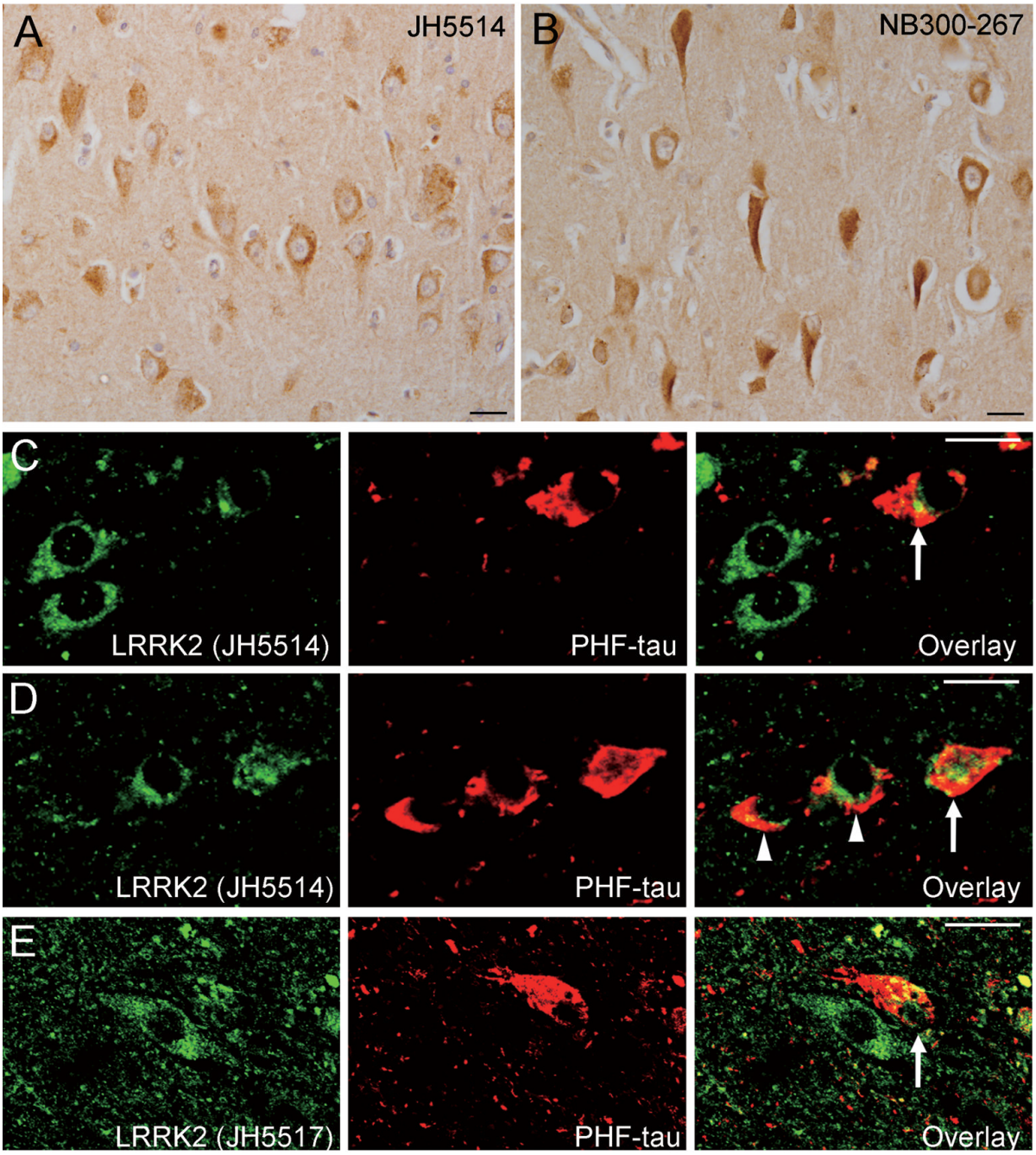

Figure 2.

Localization of leucine-rich repeat kinase 2 (LRRK2) in brains from Alzheimer disease (AD) cases. **(A, B)** LRRK2 immunoreactivity in the hippocampal CA region stained with antibody JH5514 (**A**) or NB300-267 (**B**). **(C-E)** Double immunofluorescent labeling for LRRK2 (**C, D**: JH5514, **E**: JH5517) and paired helical filament (PHF)-tau shows that LRRK2 either does not colocalize (arrowheads) or only partially colocalizes (arrows) with PHF-tau-positive neurofibrillary tangles. All scale bars = 20 μm.

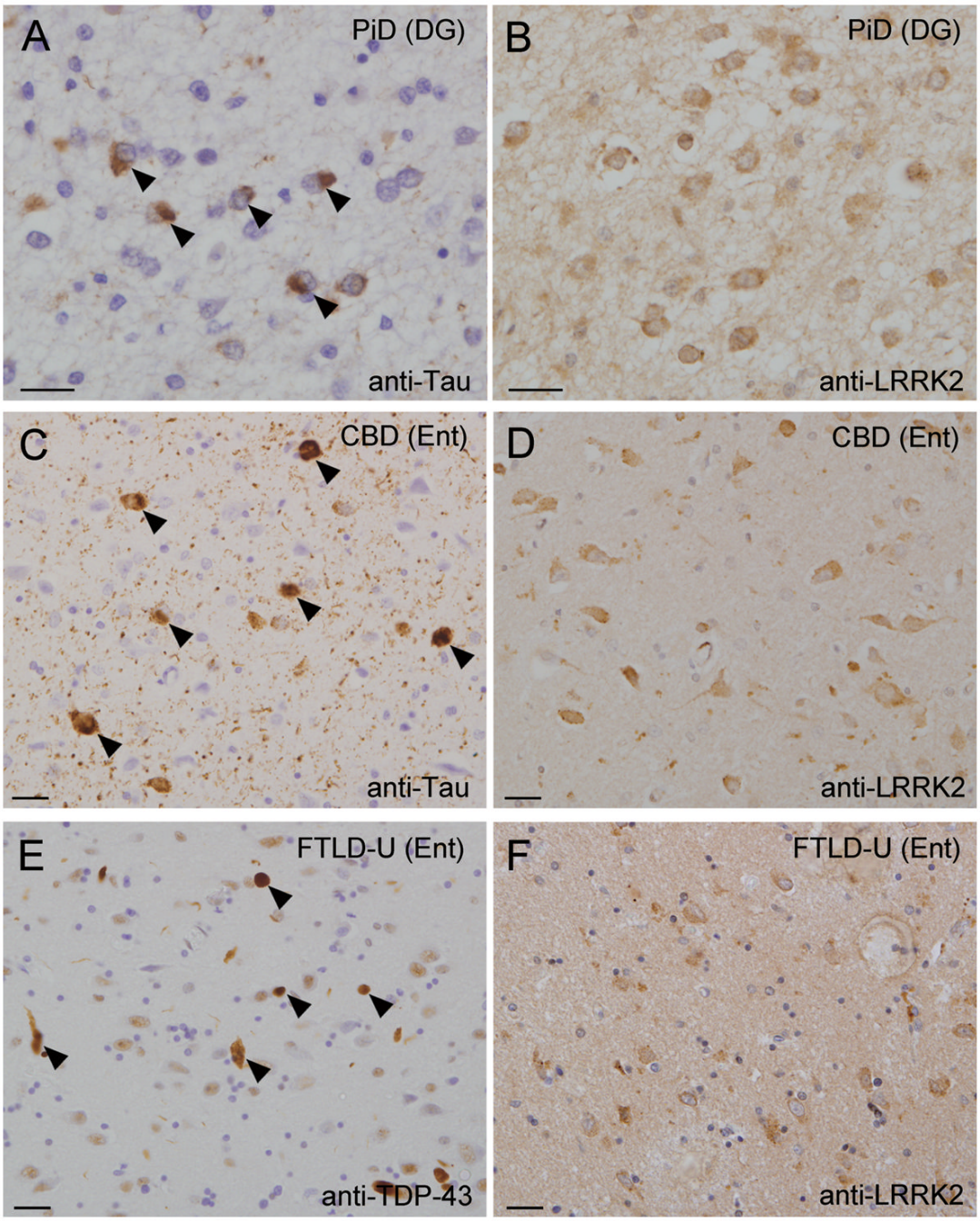

Figure 3.

Localization of leucine-rich repeat kinase 2 (LRRK2) in various neurodegenerative diseases. **(A, B)** Consecutive paired sections from the dentate gyrus (DG) of a case of Pick disease (PiD) stained with anti-paired helical filament (PHF)-tau (**A**) or anti-LRRK2, NB300-267 antibody (**B**). Arrowheads in (**A**) indicate tau-positive Pick bodies. **(C, D)** Consecutive sections from the entorhinal cortex (Ent) of a case of corticobasal degeneration (CBD) stained with anti-PHF-tau (**C**) or anti-LRRK2, NB300-267 antibody (**D**). Arrowheads in (**C**) highlight tau-positive pretangles. **(E, F)** Consecutive sections from the Ent of a case of frontotemporal lobar degeneration with ubiquitin-positive inclusions (FTLD-U) stained with anti-TAR DNA binding protein-43 (TDP-43) (**E**) or anti-LRRK2, NB300-267 antibody (**F**). Arrowheads in

(**E**) indicate TDP-43-positive dystrophic neurites. Panels A and B, C and D, and E and F are paired consecutive sections obtained from the same affected brain region of a single case for each disorder. All scale bars = 20 μm.

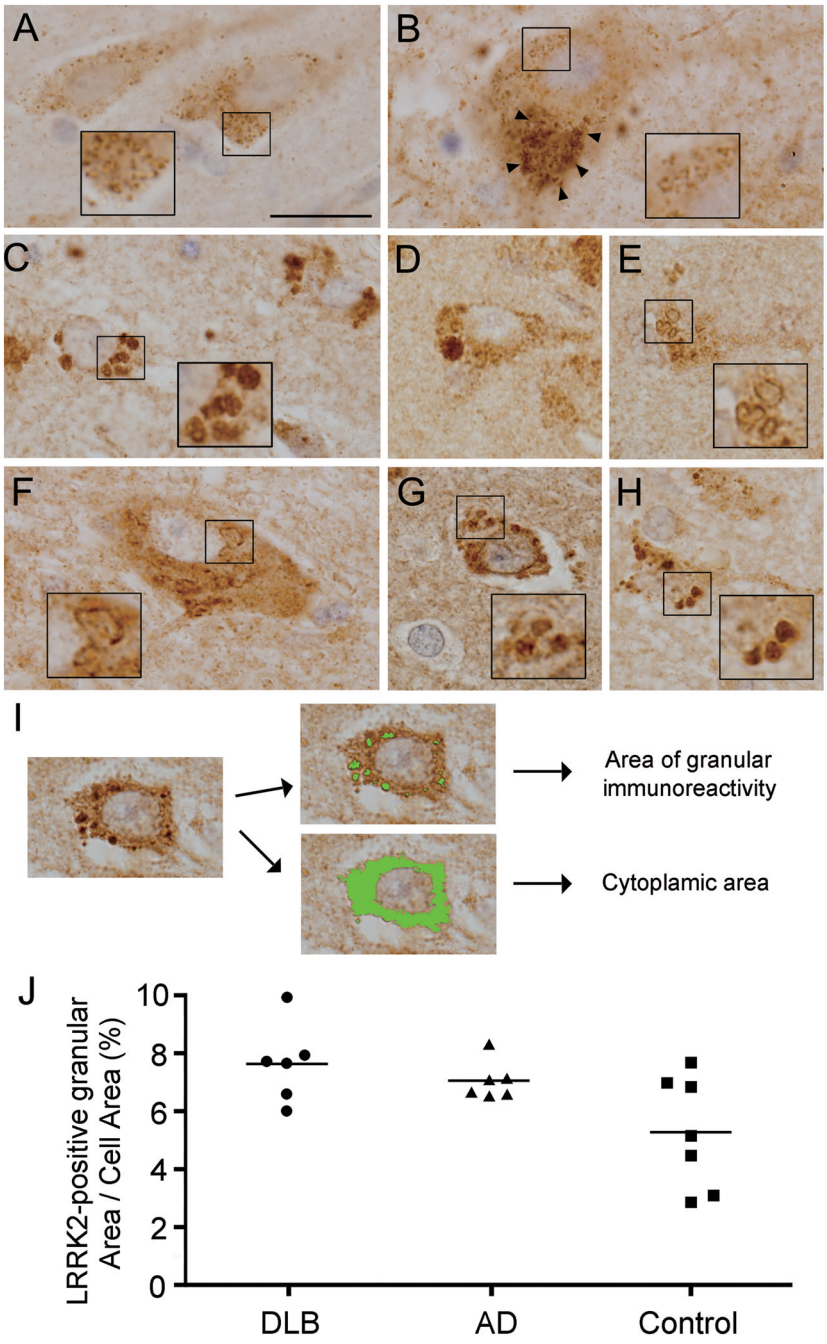

Figure 4.

Leucine-rich repeat kinase 2 (LRRK2)-positive enlarged granules and vacuoles. **(A, B)** In normal aged controls, LRRK2 immunoreactivity has a small punctate pattern throughout the neuronal soma and processes in the entorhinal cortex (**A**) or neuromelanin-containing dopaminergic neurons (arrowheads) of the substantia nigra pars compacta. **(C-E)** In the entorhinal cortex of DLB cases, LRRK2 immunoreactivity in neurons is mostly in abnormal enlarged (**C**) or giant (**D**) granules or clustered vacuoles (**E**). **(F, G)** LRRK2-positive vacuoles or granules in neurons of the substantia nigra pars compacta (**F**) and entorhinal cortex (**G**) from PD cases. **(H)** LRRK2-positive enlarged granules in neurons of the entorhinal cortex from an AD case. Scale bar in (A) represents 20 μm in A-H. **(I)** Computerized image analysis for

estimation of the volume of enlarged granules immunostained with anti-LRRK2 antibody (JH5514) or total cytoplasmic area outlined by brown (DAB) immunoreactivity, as described in Methods. **(J)** Percentage of total cell area occupied by LRRK2-positive granules in neurons of the entorhinal cortex of DLB brains (n = 6), AD brains (n = 6) and aged control brains (n = 7). Values are the mean percentage calculated from 25 neurons per brain.

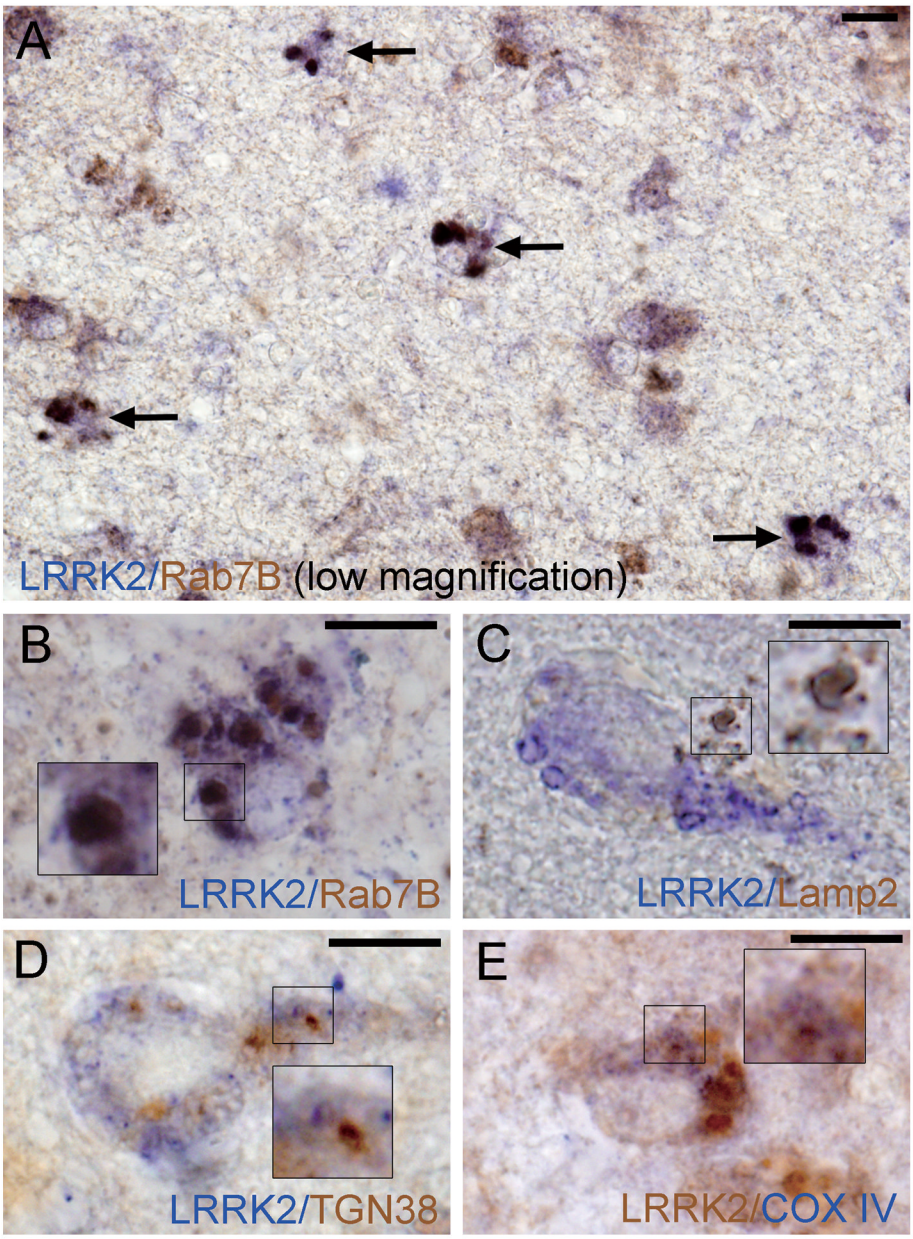

Figure 5.

Double colorimetric immunolabeling for leucine-rich repeat kinase 2 (LRRK2) and organelle markers in neurons of the entorhinal cortex from cases of Dementia with Lewy bodies (DLB). (**A, B**) Late-endosome (Rab7B); (**C**) lysosome (LAMP2); (**D**) trans-Golgi network (TGN38) (**E**) mitochondria (COX IV). Each color (brown or blue) corresponding to LRRK2 immunoreactivity or organelle maker immunoreactivity is indicated in each image. Insets in **B–E** are enlarged regions as indicated. Arrows in (**A**) highlight neurons with double-positive enlarged granules for LRRK2 and Rab7B (dark brown). LRRK2-positive granules mainly colocalize with Rab7B (**A, B**) and to a lesser extent with LAMP2 (**C**), but show minimal overlap with TGN38 (**D**) and COX IV (**E**). All scale bars = 10 μm.

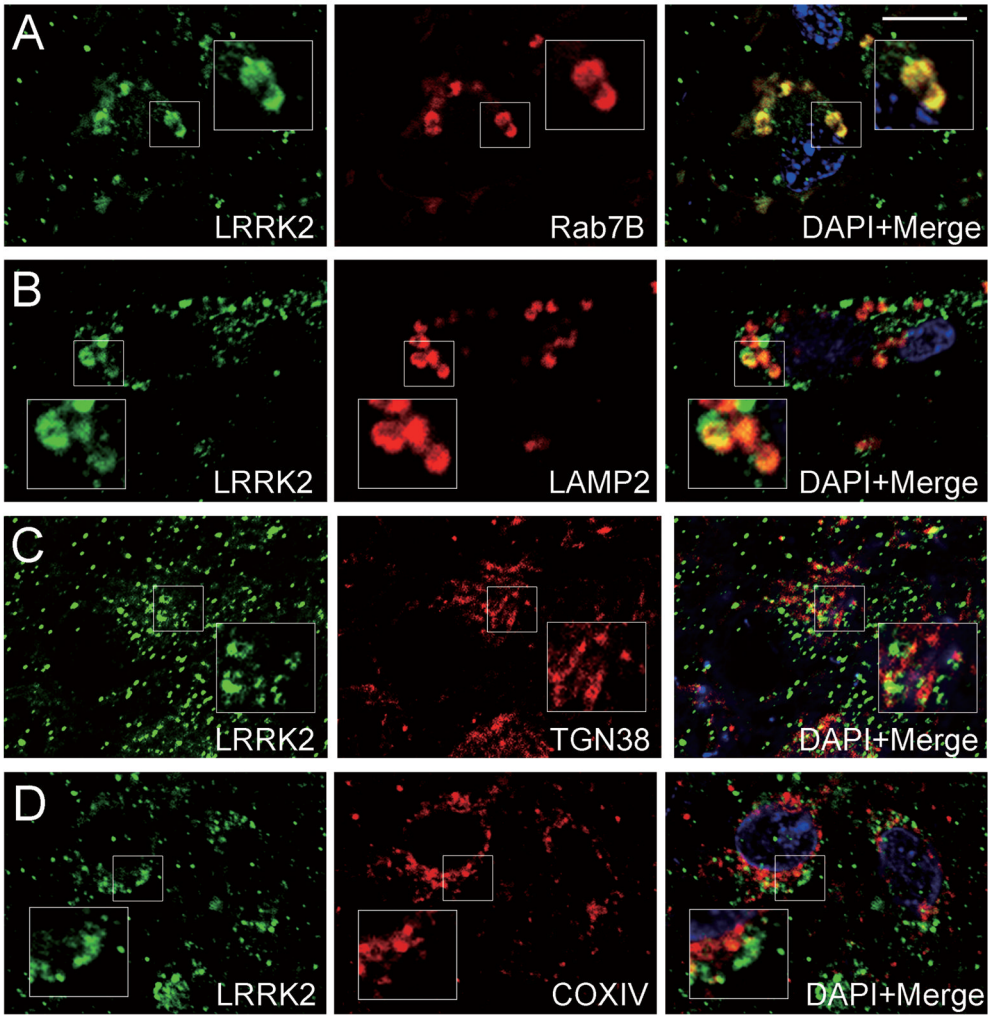

Figure 6.

Confocal double immunofluorescent images for leucine-rich repeat kinase 2 (LRRK2) and organelle markers in neurons of the entorhinal cortex from cases of Dementia with Lewy bodies (DLB). (**A**) late-endosome (Rab7B); (**B**) lysosome (LAMP2); (**C**) trans-Golgi network (TGN38); (**D**) mitochondria (COX IV). Insets in **A–D** represent enlarged regions as indicated. LRRK2-positive granules mainly colocalize with Rab7B (**A**) and to a lesser extent with LAMP2 (**B**), but show minimal overlap with TGN38 (**C**) and COX IV (**D**). Scale bar in (A) = 10 μm in A–D.

Table 1

Clinical and Demographic Data

Group	*n* (male:female)	Age (y) (mean ± SD)	Brain weight (g) (mean ± SD)	Disease duration (yrs) (mean ± SD)
PD	2 (1:1)	58 ± 19.8	1190±156	7±1.4
DLB	6 (4:2)	69.3 ± 10.6	1071±137	4.8±1.3
AD	6 (3:3)	77.3 ± 11	1080±124	7±3.7
PiD	2 (1:1)	72.5 ± 2.1	790±156	10.5±6.4
PSP	1 (1:0)	67	1160	5
CBD	1 (0:1)	72	867	16
FTLD-U	3 (2:1)	67.3 ± 3.1	1008 ± 172	8.7±3.8
Control	7 (4:3)	73.9 ± 5.2	1294 ± 34	-

PD, Parkinson disease; DLB, dementia with Lewy bodies; AD, Alzheimer disease; PiD, Pick disease; PSP, progressive supranuclear palsy; CBD, corticobasal degeneration; FTLD-U, frontotemporal lobar degeneration with ubiquitin-positive inclusions; Control, aged normal subjects. Ages, brain weights and disease durations for each group are mean ± SD

Table 2

Neuropathological Data on Parkinson Disease, Dementia with Lewy Bodies and Alzheimer Disease Cases

Case No.	Aβ stage	NF stage	Lewy stage	AD criteria	DLB criteria
PD1	B	I	I>	~	~
PD2	A	I	I>	~	~
DLB1	C	IV	IV	~	high (diffuse neocortical)
DLB2	C	II	III	~	high (diffuse neocortical)
DLB3	0	II	IV	~	high (diffuse neocortical)
DLB4	C	II	III	~	high (diffuse neocortical)
DLB5	C	II	III	~	high (diffuse neocortical)
DLB6	C	II	III	~	high (diffuse neocortical)
AD1	C	V	~	high	~
AD2	C	V	~	high	~
AD3	C	IV	~	high	~
AD4	C	V	~	high	~
AD5	C	V	~	high	~
AD6	C	V	~	high	~

Amyloid β (Aβ) stages (A–C) and neurofibrillary (NF) stages (I–VI) were determined according to Braak staging (33). Lewy stages (I-IV) in DLB were assigned according to our previous protocol (34). Consensus criteria were used to diagnose PD (29), DLB (30) and AD (31). PD, Parkinson disease; DLB, dementia with Lewy bodies; AD, Alzheimer disease; ~, not applicable.

Table 3

Antibodies

Antibody	Type, Species	Source and reference	Staining Dilution
Anti-LRRK2 (JH5514)	polyclonal, rabbit	In-house (Johns Hopkins)	1:400
Anti-LRRK2 (JH5517)	polyclonal, rabbit	In-house (Johns Hopkins)	1:400
Anti-LRRK2 (NB300-267)	polyclonal, rabbit	Novus Biologicals, Littleton, CO (19)	1:400
Anti- Phosphorylated α-synuclein (Pser129)	monoclonal, mouse	Gift from Dr. T. Iwatsubo, University of Tokyo, Tokyo, Japan (39)	1:20,000
Anti-Amyloid β	polyclonal rabbit	Gift from Dr. T. Ishii, (Sagamidai Hospital, Kanagawa, Japan)	1:5000
Anti-PHF tau (AT8)	monoclonal, mouse	Innogenetics, Zwijnaarde, Belgium	1:2000
Anti-TDP-43 (10782-1-AP)	polyclonal, rabbit	ProteinTech Group, Chicago, IL	1:2000
Anti-LAMP2 (H4B4)	monoclonal, mouse	Santa Cruz Biotechnology, Santa Cruz, CA	1:200
Anti-Rab7B (3B3)	monoclonal, mouse	Abnova Corporation, Taipei, Taiwan	1:200
Anti-COX IV	monoclonal, mouse	Abcam, Tokyo, Japan	1:400
Anti- TGN38/TGOLN2 (M02)	monoclonal, mouse	Abnova Corporation, Taipei, Taiwan	1:200

PHF, paired helical filaments; TDP-43, TAR-DNA binding protein-43; COX IV, LAMP2, lysosomal-associated membrane protein 2; cytochrome oxidase c subunit TGOLN2, trans-golgi network protein 2.